

The structure of Ge₂Sb₂Te₅ and the mechanism of its rapid phase change

S. Kohara^a, K. Ohara^a, L. Temleitner^a, K. Kobayashi^b, J. Akola^{c,d,e}, R. O. Jones^{e,f},
T. Matsunaga^g, R. Kojima^g, N. Yamada^g, and M. Takata^{h,i}

^aSPring-8/JASRI, 1-1-1 Kouto, Sayo-cho, Sayo-gun, Hyogo 679-5198, Japan

^bBeamline Station at SPring-8, National Institute for Materials Science, 1-1-1 Kouto, Sayo-gun, Hyogo 679-5198, Japan

^cDepartment of Physics, Tampere University of Technology, P.O. Box 692, FI-33101 Tampere, Finland

^dNanoscience Center, Department of Physics, University of Jyväskylä, P.O. Box 35, FI-40014 Jyväskylä, Finland

^eInstitut für Festkörperforschung, Forschungszentrum Jülich, D-52425 Jülich, Germany

^fGerman Research School for Simulation Sciences, FZ Jülich and RWTH Aachen University, D-52425 Jülich, Germany

^gPanasonic Corporation, 3-1-1 Yagumo-Nakamachi, Moriguchi, Osaka 570-8501 Japan

^hSPring-8/RIKEN, 1-1-1 Kouto, Sayo-cho, Sayo-gun, Hyogo 679-5148, Japan

ⁱDepartment of Advanced Materials Science, School of Frontier Science, The University of Tokyo, 5-1-5, Kashiwanoha, Chiba 277-8561, Japan

ABSTRACT

We have determined the crystalline and amorphous phases of GST using a combination of advanced synchrotron radiation experiments and massively parallel molecular dynamics (MD) / density functional (DF) simulations and reverse Monte Carlo (RMC) methods. We focus on the structural similarity of the two phases, paying particular attention to the bond angles (defined by three atoms) and the ring statistics (connectivity of atoms) beyond the nearest neighbors. Furthermore, we address the relationship between bond recombination and phase change speed.

INTRODUCTION

Since its discovery in 1987,¹⁾ much work has been carried out on the structure of Ge₂Sb₂Te₅ (GST) and the reasons for its rapid phase change. The “umbrella flip model” proposed by Kolobov et al.,²⁾ in particular, led to some controversy and to the recognition that knowledge of the structure of amorphous GST was crucial. Many experiments and computer simulations have addressed this problem.³⁾

To understand the structure of Ge₂Sb₂Te₅ and the mechanism of its rapid phase change, we have used a combination of theory and experiment. We have performed synchrotron x-ray diffraction (XRD) measurements^{4,5)} and x-ray photoelectron spectroscopy (XPS) measurements⁶⁾ on both

crystal and amorphous $\text{Ge}_2\text{Sb}_2\text{Te}_5$ and have performed a very extensive density functional theory (DF) / molecular dynamics (MD) simulation on 460 particles⁷⁾ to obtain a model of the amorphous phase. This model was recently refined on the basis of reverse Monte Carlo simulation (RMC) to reproduce both XRD and XPS data.⁸⁾ Here we apply RMC simulation techniques to the crystal phase of $\text{Ge}_2\text{Sb}_2\text{Te}_5$ (rock salt structure) and compare the three-dimensional configurations of the amorphous and crystal phases of $\text{Ge}_2\text{Sb}_2\text{Te}_5$ at intermediate range by deriving bond angle distributions and ring statistics, i.e. the atomic connectivity. We discuss the relationship between bond recombination and the speed of phase change.

EXPERIMENTS

Sample preparation

The specimen for high-energy x-ray diffraction experiments was made by laminating an organic film sheet on a glass disc with a diameter of 120 mm and sputtering to form the recording film with a thickness of 200 – 500 nm. The organic film was scraped from the glass disc, and the specimen was removed from the glass substrate using a spatula. The composition of the sample was examined by inductively coupled plasma atomic emission spectrometry. The 300-nm thick samples for time-resolved x-ray diffraction experiments were prepared by depositing $\text{Ge}_2\text{Sb}_2\text{Te}_5$ on a SiO_2 glass substrate (12 cm diameter and 0.6 mm thick) with a 2-nm thick 80 mol% ZnS-20 mol% SiO_2 cap layer.

High-energy x-ray diffraction experiment

The high-energy x-ray diffraction experiment was carried out at the high-energy x-ray diffraction beamline BL04B2.⁹⁾ The diffraction patterns of powder sample in a thin walled (10 μm) tube of 0.5 mm diameter (supplier: GLAS Müller, D-13503 Berlin) and an empty tube were measured in a transmission geometry. The collected data were corrected using standard programs,⁹⁾ and the corrected data were normalized to give the coherent scattering intensity $I(Q)$ and the Faber-Ziman structure factor $S(Q)$.¹⁰⁾

RMC simulation

The RMC method¹¹⁾ is a useful tool for constructing three-dimensional structural models of disordered materials using mainly experimental diffraction data. In this technique, the atoms of an initial configuration are moved to minimize the deviation from experimental diffraction and/or EXAFS data. This technique has been applied extensively to disordered materials that do not exhibit structural periodicity¹²⁾ and to crystalline materials to understand local structure and disorder.^{13,14)} In

this study, we have applied the RMCPOW code¹³⁾ to the metastable cubic phase to derive a 3-dimensional atomic configuration. A 10 x 10 x 10 supercell configuration of 7200 particles was used to fit the coherent scattering intensity $I(Q)$. The Sb and Ge atomic positions were interchanged during the simulation.

RESULTS

It is well known that crystalline $\text{Ge}_2\text{Sb}_2\text{Te}_5$ has a rock salt (NaCl-type) structure with 20% vacancies and random Ge/Sb occupation of one sublattice.⁴⁾ Figure 1 shows the coherent scattering intensity $I(Q)$ obtained by RMC simulations. The agreement between experimental data and the RMC model is excellent.

The partial pair correlation functions, $g_{ij}(r)$, of crystal $\text{Ge}_2\text{Sb}_2\text{Te}_5$ (c-GST) obtained from the RMC model are shown in Fig. 2 together with the data of amorphous $\text{Ge}_2\text{Sb}_2\text{Te}_5$ (a-GST).⁸⁾ It is remarkable that c-GST exhibits significant oscillations indicating long-range periodicity in the crystal phase. The most striking feature in a-GST is that both Ge-Te and Sb-Te exhibit a well defined first peak whose amplitude is comparable to those of c-GST. This feature shows that AB ($A=\text{Ge}, \text{Sb}$, $B=\text{Te}$) alternation is significant in a-GST, which is an important feature of this material. However, the positions of Ge-Te and Sb-Te correlation peaks in a-GST are smaller than those in c-GST, suggesting that both Ge-Te and Sb-Te form covalent bonds with smaller coordination numbers in the amorphous phase.

Figure 3 shows bond angle distributions of Te-Ge-Te and Te-Sb-Te in c-GST and a-GST. Crystalline GST shows a well-defined peak at 90 degrees arising from the rock salt structure. The bond angle distributions of Te-Ge-Te and Te-Sb-Te in a-GST are similar to those of c-GST, although the peak width in a-GST is slightly larger than in c-GST.

The ring statistics, which show the connectivity of Ge-Te and Sb-Te, is an important structural parameter for understanding the similarity between c-GST and a-GST. The calculation used the *shortest-path* analysis, where we count the number of atoms in the shortest closed loop from a given atom. The calculated ring statistics for c-GST and a-GST are shown in Fig. 4, where $A-B-A-B$ rings are fourfold rings found in the NaCl lattice. As can be seen in the figure, c-GST consists of four- and sixfold rings due to the 20% vacancies on 4(*a*) sites. On the other hand, a-GST has a significant number of fourfold rings, which can be recognized as nuclei of crystal. This feature can be seen clearly in Fig. 5, where structural units found in the NaCl lattice are evident. These results suggest that the similarity of bond angle distribution and ring statistics in c-GST is a-GST is a unique feature of GST. Furthermore we propose that the numerous 4-fold rings with $ABAB$ alternation ($A: \text{Ge}, \text{Sb}$;

B: Te) is the key to the rapid crystallization of a-GST, since such fourfold rings can act as nuclei, and the presence of many four- and sixfold rings (see. Fig. 4) allows the phase change to occur with less bond breaking and formation.

CONCLUSIONS

We have applied RMC simulation to synchrotron x-ray diffraction data on crystalline Ge₂Sb₂Te₅ and have compared the results with those of amorphous phase. The structures of c-GST and a-GST have similar bond angle distributions and ring statistics. Furthermore, a-GST has numerous fourfold rings with *ABAB* alternation (*A*: Ge, Sb; *B*: Te). We propose that they act as nuclei in the rapid phase-change to the NaCl crystalline phase and that this feature is the basis of rapid nucleation driven crystallization with little bond breaking and formation.

ACKNOWLEDGEMENTS

We thank Prof. László Pusztai for fruitful discussions. This work was supported by CREST “X-ray pinpoint structural measurement project - Development of the spatial- and time-resolved structural study for nano-materials and devices” and the Academy of Finland and the Japan Science and Technology Agency via the Strategic Japanese-Finland Cooperative Program on “Functional Materials”. The MD/DF simulations were performed on the Jugene (IBM BlueGene/P) supercomputer in the Forschungszentrum Jülich with grants from the FZJ and the John von Neumann Institute for Computing (NIC).

REFERENCES

1. N. Yamada et al., Jpn. J. Appl. Phys. **26**, Suppl. 26–4, 61 (1987).
2. A. Kolobov et al., Nature Mater. **3**, 703 (2004).
3. M. Wuttig and N. Yamada, Nature Mater. **6**, 824 (2007).
4. N. Yamada and T. Matsunaga, J. Appl. Phys. **88**, 7020 (2000).
5. S. Kohara et al., Appl. Phys. Lett. **89**, 201910 (2006).
6. J. J. Kim et al., Phys. Rev. B **76**, 115214 (2007).
7. J. Akola and R. O. Jones, Phys. Rev. B **76**, 235201 (2007).
8. J. Akola et al., Phys. Rev. B **80**, 020201R (2009).
9. S. Kohara et al., J. Phys.: Condens. Matter **19**, 506101 (2007).
10. T. E. Faber and J. M. Ziman, Philos. Mag. **11**, 153 (1965).
11. R. L. McGreevy and L. Pusztai, Mol. Simul. **1**, 359 (1988).

12. R. L. McGreevy, J. Phys.: Condens. Matter **13**, R877 (2001).
13. A. Møllergård, R. L. McGreevy, Acta Cryst. **A55**, 783 (1999).
14. M. Tucker et al.: J. Phys.: Condens. Matter **19**, 335218 (2007).

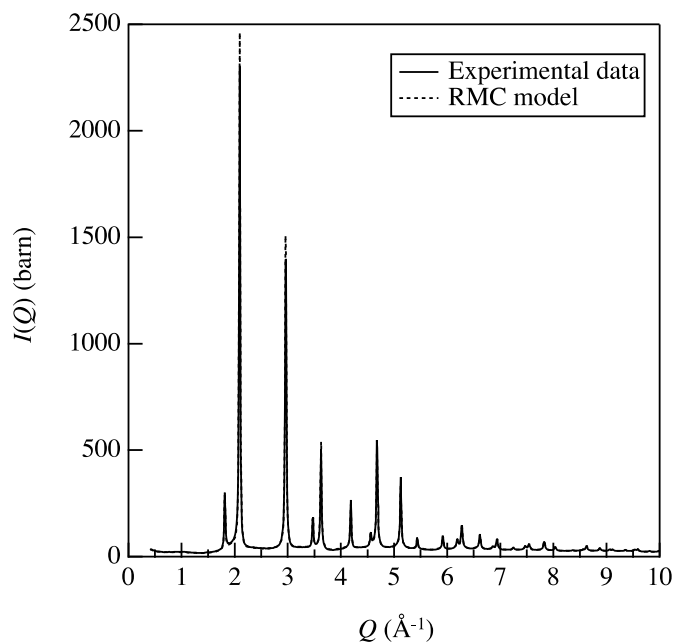


Fig. 1 Normalized x-ray scattering intensity $I(Q)$ for c-GST.

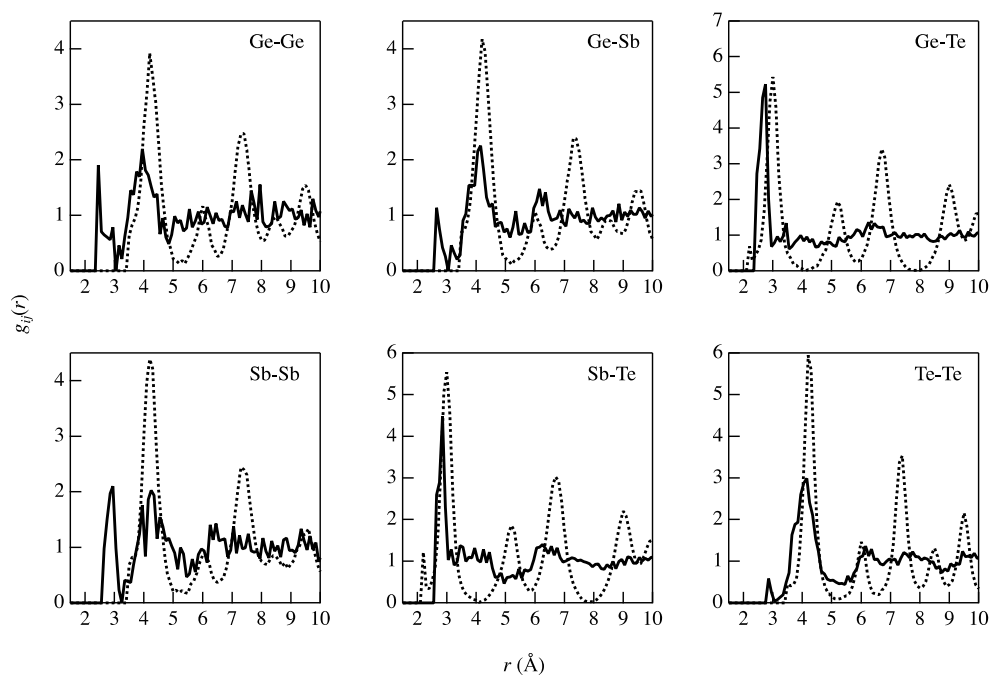


Fig. 2 Partial pair correlation function $g_{ij}(r)$ for c-GST (dotted lines) and a-GST (solid lines).

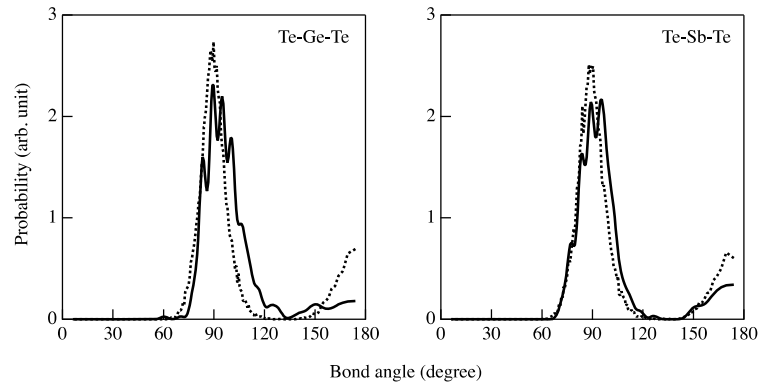


Fig. 3 Bond angle distributions for c-GST(dotted lines) and a-GST (solid lines).

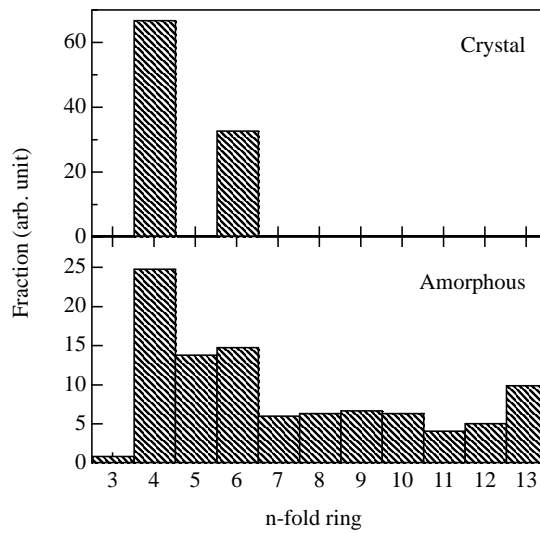


Fig. 4 Ring statistics for c-GST and a-GST.

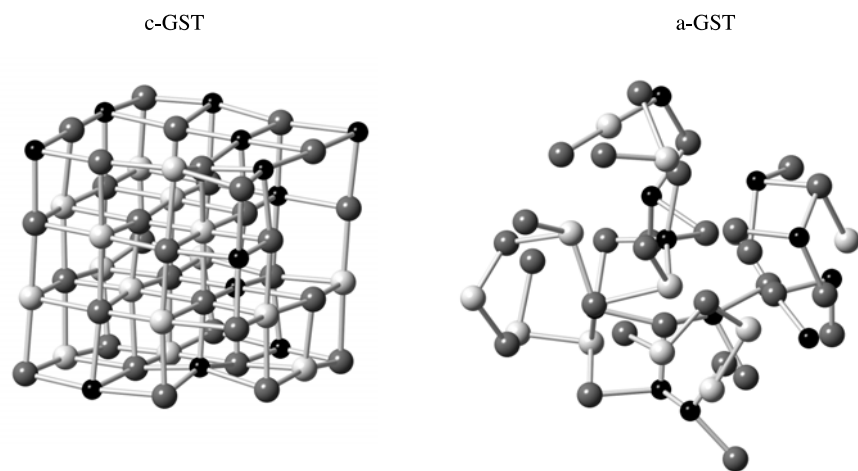


Fig. 5 Atomic configuration of c-GST and a-GST obtained from RMC simulation.